Competing Roles of Aldo-Keto Reductase 1A1 and Cytochrome P4501B1 in Benzo[a]pyrene-7,8-diol Activation in Human Bronchoalveolar H358 Cells: Role of AKRs in P4501B1 Induction

ARTICLE *in* CHEMICAL RESEARCH IN TOXICOLOGY · FEBRUARY 2006

Impact Factor: 3.53 · DOI: 10.1021/tx0502488 · Source: PubMed

4 AUTHORS, INCLUDING:

Hao Jiang
Bristol-Myers Squibb
40 PUBLICATIONS **475** CITATIONS
SEE PROFILE

Daljit Vudathala
University of Pennsylvania
14 PUBLICATIONS **273** CITATIONS
SEE PROFILE

Ian A Blair
University of Pennsylvania
430 PUBLICATIONS **12,506** CITATIONS
SEE PROFILE

Competing Roles of Aldo-Keto Reductase 1A1 and Cytochrome P4501B1 in Benzo[*a*]pyrene-7,8-diol Activation in Human Bronchoalveolar H358 Cells: Role of AKRs in P4501B1 Induction

Hao Jiang,[†] Daljit K. Vudathala,[‡] Ian A. Blair,[‡] and Trevor M. Penning*[,†]

Department of Pharmacology and Center for Cancer Pharmacology, University of Pennsylvania School of Medicine, Philadelphia, Pennsylvania 19104-6084

Received September 8, 2005

Benzo[*a*]pyrene (BP) requires metabolic activation to electrophiles to exert its deleterious effects. We compared the respective roles of aldo-keto reductase 1A1 (AKR1A1, aldehyde reductase) and P4501B1 in the formation of BP-7,8-dione and BP-tetrols, respectively, in intact bronchoalveolar cells manipulated to express either enzyme. Metabolite formation was confirmed by HPLC/MS and quantitatively measured by HPLC/UV/β-RAM. In TCDD-treated H358 cells (P4501B1 expression), the *anti*-BPDE hydrolysis product BP-tetrol-1 increased over 3−12 h to a constant level. In H358 AKR1A1 transfectants, formation of BP-7,8-dione was elevated for 3−12 h but significantly decreased after 24 h. Interestingly, BP-tetrols were also detected in AKR1A1 transfectants even though they do not constitutively express P4501A1/P4501B1 enzymes. Northern and Western blotting confirmed the induction of P4501B1 by BP-7,8-dione in parental cells and the induction of P4501B1 by BP-7,8-diol in AKR1A1-transfected cells. P4501B1 induction was blocked in AKR1A1 transfectants by the AKR1A1 inhibitor (sulfonylnitromethane), the *o*-quinone scavenger (*N*-acetyl-L-cysteine), or the cytosolic AhR antagonist (diflubenzuron). Attenuation of P4501B1 induction in these cells was verified by measuring a decrease in BP-tetrol formation. Our studies show that the formation of BP-7,8-dione by AKR1A1 in human bronchoalveolar cells leads to an induction of P4501B1 and that a functional consequence of this induction is elevated *anti*-BPDE production as detected by increased BP-tetrol formation. Therefore, the role of AKR1A1 in the activation of BP-7,8-diol is bifunctional; that is, it directly activates BP-7,8-diol to the reactive and redox-active PAH *o*-quinone (BP-7,8-dione) and it indirectly trans-activates the *P4501B1* gene by generating the aryl hydrocarbon receptor (AhR) ligand BP-7,8-dione.

Introduction

Polycyclic aromatic hydrocarbons (PAHs)[1] (e.g., benzo[*a*]pyrene and benz[*a*]anthracene) are ubiquitous environmental pollutants. They are found in tobacco smoke and are implicated in the causation of human lung cancer (*1*). To exert their carcinogenic effects, PAH must be activated to electrophilic metabolites. Three proposed pathways of metabolic activation have been proposed, that is, the P450 peroxidase pathway resulting in the formation of radical cations (*2*), the P4501A1/P4501B1/epoxide hydrolase (EH) pathway resulting in the formation of diol-epoxides, for example, (±)-*trans*-7,8-dihydroxy-9α,10α-epoxy-7,8,9,10-tetrahydrobenzo[*a*]pyrene (*anti*-BPDE) (*3*−*4*), and the aldo-keto reductase (AKR) pathway (human AKR1A1, AKR1C1−AKR1C4) resulting in the formation of PAH *o*-quinones and reactive oxygen species (ROS) (*5*). Importantly, P4501A1/1B1 and aldo-keto reductases (AKR1A1 and AKR1C1−1C4) play competing roles in the metabolic activation of the proximate carcinogen (−)-BP-7,8-diol to generate either the electrophilic *anti*-BPDE or the chemically reactive and redox-active PAH *o*-quinone (BP-7,8-dione), Figure 1.

The role of the P4501A1/1B1 pathway in the generation of *anti*-BPDE has been well-studied. *Anti*-BPDE is one of the most mutagenic metabolites of BP in bacterial and mammalian cell assays (*6*−*8*) and is the most tumorigenic metabolite in causing pulmonary adenomas in mice (*9*−*11*). These properties result from the formation of stable DNA adducts with deoxyguanosine (dGuo) and deoxyadenosine (dAdo) (*12*−*14*). Furthermore, *anti*-BPDE will activate the c-H-*ras*-1 proto-oncogene to transform NIH/3T3 cells (*15*). This gain in function results from a single point mutation in the 12th codon of *ras* in which there is a G to T transversion. Reaction of *anti*-BPDE with the *p53* tumor suppressor gene leads to adduct formation in codons 157, 158, 179, 248, and 273. These codons correspond to hot spots that are mutated in lung cancer patients, and the resultant G to T transversions lead to *p53* inactivation (*16*−*17*). Thus, *anti*-BPDE

* To whom correspondence should be addressed. Tel: 215-898-9445. Fax: 215-573-2236. E-mail: penning@pharm.med.upenn.edu.

[†] Department of Pharmacology, University of Pennsylvania School of Medicine.

[‡] Center for Cancer Pharmacology, University of Pennsylvania School of Medicine.

[1] Abbreviations: AhR, aryl hydrocarbon receptor; AKRs, aldo-keto reductases, including AKR1A1 (human aldehyde reductase), AKR1C1−AKR1C4; Arnt, AhR-nuclear translocator BA, benz[*a*]anthracene; BP, benzo[*a*]pyrene; BP-7,8-diol, (±)-*trans*-7,8-dihydroxy-7,8-dihydrobenzo-[*a*]pyrene; BP-7,8-dione, benzo[*a*]pyrene-7,8-dione; (±)-*anti*-BPDE, (±)-*trans*-7,8-dihydroxy-9α,10α-epoxy-7,8,9,10-tetrahydrobenzo[*a*]pyrene; dAdo, deoxyadenosine; dGuo, deoxyguanosine; DFB, diflubenzuron; DPBS, Dulbecco's phosphate-buffered saline; ECL, enhanced chemiluminescence; EH, epoxide hydrolase; ESI, electrospray; GAPDH, glucose 6-phosphate dehydrogenase; MAPK, mitogen activated protein kinase; NAC, *N*-acetyl-L-cysteine; 8-oxo-dGuo, 8-oxo-2-deoxyguanosine; PAHs, polycyclic aromatic hydrocarbons; P4501A1/P4501B1, cytochrome P4501A1 or cytochrome P4501B1; PKC, protein kinase C; ROS, reactive oxygen species; SDS−PAGE, sodium dodecyl sulfate−polyacrylamide gel electrophoresis; SNM, Sulfonylnitromethane; tetrol-1, *r*-7,*t*-8,*t*-9,*c*-10-benzo[*a*]pyrene-tetrahydrotetrol; tetrol-2, *r*-7,*t*-8,*t*-9,*t*-10-benzo[*a*]pyrene-tetrahydrotetrol; tetrol-3, *r*-7,*t*-8,*c*-9,*c*-10-benzo[*a*]pyrene-tetrahydrotetrol; tetrol-4, *r*-7,*t*-8,10,*c*-9-benzo[*a*]pyrene-tetrahydrotetrol; TCDD, 2,3,7,8-tetrachlorodibenzo-*p*-dioxin; TMS, tetramethoxy stilbene; XRE, xenobiotic response element.

10.1021/tx0502488 CCC: $33.50
Published on Web 12/17/2005

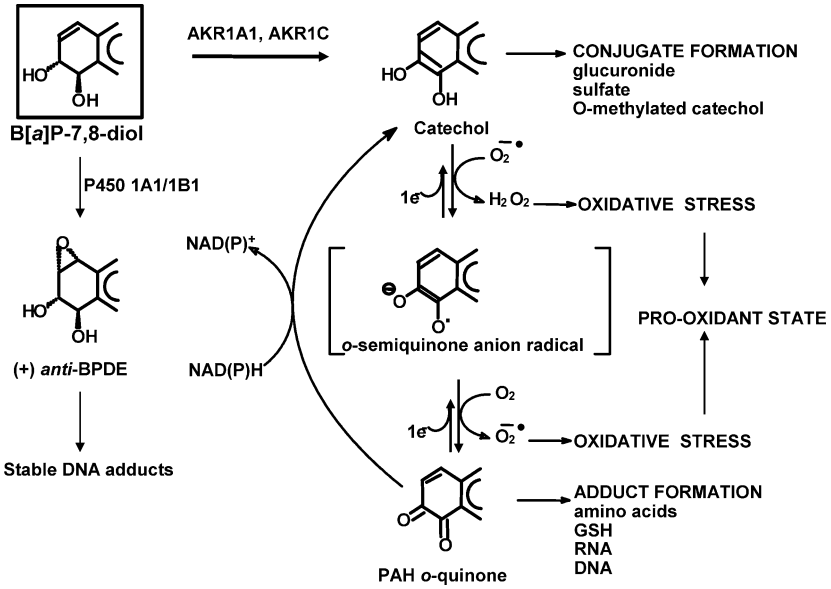

Figure 1. Metabolic activation of PAH *trans*-dihydrodiols by AKR isoforms and P4501A1/P4501B1.

can mutate oncogenes and tumor suppressor genes associated with human lung cancer.

In contrast, the AKR pathway leads to the oxidation of (−)-BP-7,8-diol to form the resultant ketol that rearranges to a catechol. The catechol undergoes two one-electron autoxidation events with the concomitant production of reactive oxygen species to form PAH *o*-quinones (*5*). Once formed, PAH *o*-quinones undergo conjugation reactions with endogenous nucleophiles (L-cysteine, *N*-acetyl-L-cysteine, GSH, etc.), which can lead to a depletion of cellular reducing equivalents and lead to a change in redox state (*18*). PAH *o*-quinones are also reactive Michael acceptors which can react with DNA to form either stable bulky adducts or depurinating adducts (*19*−*21*), which may provide routes to G to T transversions and change-in-function gene mutations.

In the presence of cellular reducing equivalents, for example, NADPH, PAH *o*-quinones can also be reduced back to the catechol establishing futile redox cycles which generate ROS. PAH *o*-quinones under redox-cycling conditions cause the formation of oxidatively damaged bases, for example, 8-oxo-dGuo (*22*), which if unrepaired could mismatch with A on the replicative strand, leading to G to T transversions (*23*). ROS can also lead to elevated levels of lipid peroxidation, inducing the formation of 4-hydroperoxy-2-nonenal (HPNE) (*24*), 4-hydroxy-2-nonenal (HNE) (*25*), and 4-oxo-2-nonenal (ONE) (*26*), which can form dihydroxyheptane-etheno− (*27*−*29*) and heptanone-etheno−DNA adducts (*30*−*33*). PAH *o*-quinones under redox-cycling conditions can cause DNA strand scission (*34*), and ROS can cause illegitimate recombination (*35*−*36*). In addition, the pro-oxidant state produced may cause already initiated cells to expand and modulate protein kinase C to enhance tumor promotion (*37*−*38*). It is highly likely that generation of PAH *o*-quinones and ROS via the AKR pathway contributes to the initiation and promotion phases of PAH carcinogenesis.

The respective contribution of the P450 and AKR pathways to PAH activation remains to be fully elucidated. Multiple human tissue expression array analysis showed coexpression of AKR1A1, P4501A1/1B1, and EH in human tissues, indicating that *trans*-dihydrodiol substrates are formed in the same tissues in which AKR1A1 and P4501A1/1B1 are both expressed (*39*). Earlier studies in lysates from human bronchoalveolar cells manipulated to express both these pathways showed that BP-7,8-dione generated via the AKR1A1 pathway could be trapped by 2-mercaptoethanol in situ and that the amount of BP-7,8-dione generated was governed by the redox state (*40*). We now extend these studies to the intact human bronchoalveolar H358 cells to dissect the competing roles of AKR1A1 and P4501B1 in BP-7,8-diol activation. The competitive activation of BP-7,8-diol by AKR1A1 and P4501B1 in the cell culture models was confirmed by quantitative detection and LC/MS analysis of the metabolites. The detection of BP-tetrols in AKR1A1 transfectants in the absence of constitutively expressed P450 provided evidence that the AKR product BP-7,8-dione induced P4501B1 with a subsequent functional consequence on PAH metabolism.

Materials and Methods

Chemical and Reagents. Cell culture media and reagents were obtained from Invitrogen Co. (Carlsbad, CA). (±)-[1,3-^{3}H]-BP-7,8-diol (sp. act. 1170 mCi/mmol, ≥98% pure by HPLC) and unlabeled (±)-BP-7,8-diol, BP-7,8-dione, (±)-*anti*-BPDE, *r*-7,*t*-8,*t*-9,*c*-10-B[*a*]P-tetrahydrotetrol (BP-tetrol-1), *r*-7,*t*-8,*t*-9,*t*-10-B[*a*]P-tetrahydrotetrol (BP-tetrol-2), *r*-7,*t*-8,*c*-9,*c*-10-B[*a*]P-tetrahydrotetrol (BP-tetrol-3), and *r*-7,*t*-8,10,*c*-9-B[*a*]P-tetrahydrotetrol (BP-tetrol-4), and TCDD were obtained from the NCI Chemical Carcinogen Standard Reference Repository (Midwest Research Institute, Kansas City, MO). Sulfonylnitromethane (SNM) was obtained from Zeneca Pharmaceuticals (Cheshire, U.K.). *N*-acetyl-L-cysteine (NAC), diflubenzuron (DFB), and tetramethoxystilbene (TMS) were purchased from Sigma-Aldrich (St. Louis, MO). The purity and identity of all unlabeled PAH metabolites were checked by LC/MS. All solvents were HPLC grade, and all other chemicals used were of the highest grade available.

Cell Culture and Culture Model Preparations. Human bronchoalveolar H358 cells were obtained from the American Type Culture Collection (ATCC no. CRL-5807) and maintained in RPMI 1640 nutrient mixture with 10% heat-inactivated fetal bovine serum, 1% L-glutamine, and 100 units/mL of penicillin/streptomycin. Cells were incubated at 37 °C in a humidified atmosphere containing 5% CO_2 and were passaged every 4 days at a 1:3 dilution. AKR1A1 transfectants (AKR1A1$^+$/P4501B1$^-$) were obtained by stable transfection of AKR1A1-cDNA [pcDNA3.1(−)/AKR1A1 (GenBank accession number: NM_006066, −15 to +985 bp)] as described (*40*). The presence of 0.4 mg/mL G418 in culture media maintained selection pressure. P4501B1-positive cells (AKR1A1$^-$/P4501B1$^+$)

were obtained by induction with 2,3,7,8-tetrachlorodibenzo-*p*-dioxin (TCDD, 10 nM) for 12 h. Cells expressing both enzymes (AKR1A1$^+$/P4501B1$^+$) were obtained by treating AKR1A1 transfectants with TCDD.

RNA Isolation and Northern Analysis. Cellular RNA was isolated from 2×10^7 cells using Trizol reagent. Total RNA (20 μg) was separated by electrophoresis on 1% agarose/formaldehyde gels and transferred overnight to the Hybond-N$^+$ nylon membrane (Amersham Biosciences, U.K. Ltd., Little Chalfont, Bucks, U.K.). The membrane was hybridized to a cDNA probe either containing the entire open reading frame of AKR1A1 (GenBank accession number: NM_006066, −15 to +985 bp) fragment, or human P4501A1 (GenBank accession number: NM_000499, +1558 to +2602 bp, phP1-450-3′, ATCC no. 57259) or human P4501B1 (GenBank accession number: NM_000104, +2407 to +3448 bp) fragment. Random priming was conducted with radio-labeled [^{32}P]-α-dCTP, and a final specific activity greater than 10^9 cpm/μg of DNA fragment was obtained. Hybridization was performed in ExpressHyb hybridization solution (ClonTech) at 65 °C for 1 h, and the blot was subjected to a wash with 2× SSC/0.1% SDS for 20 min at room temperature and a wash with 0.2× SSC/0.1% SDS for 30 min at 60 °C. The blot was then exposed to X-ray film at −80 °C overnight. For normalization, the blot was stripped and reprobed with a 780-bp *Pst*I/*Xba*I fragment of GAPDH labeled by random priming as described above.

Immunoblot Analysis. Confluent cells (~2×10^7) were washed with 10 mL of Dulbecco's phosphate-buffered saline (DPBS) three times, harvested by scraping, and centrifuged at 800*g* for 10 min. The cells were homogenized in a glass Duall homogenizer with 200 μL of lysis buffer containing 50 mM Tris-HCl, pH 7.4, 150 mM NaCl, 1% Triton X-100, 1% sodium deoxycholate, 0.1% SDS, and protease inhibitors (1 tablet/10 mL, Roche Applied Science, Inc.), followed by centrifugation at 10 000*g* for 20 min at 4 °C. A 60-μg aliquot of the lysate supernatant or varied amounts of AKR1A1 or P4501B1 recombinant enzymes were boiled for 5 min and cooled on ice. Proteins were separated by SDS−PAGE and electrotransferred to nitrocellulose membranes (Bio-Rad Laboratories, Hercules, CA). Membranes were incubated with either polyclonal rabbit anti-human AKR1A1 antiserum (provided by Dr. John Hayes at the University of Dundee), at a 1:2000 dilution, or rabbit anti-human P4501B1 antiserum (GenTest, Woburn, MA), at a 1:2000 dilution. The immunoblots were developed by incubation with the goat anti-rabbit IgG−horseradish peroxidase conjugate as secondary antibody followed by ECL detection (Amersham Biosciences, Piscataway, NJ). The amounts of AKR1A1 and P4501B1 in cell lysates were estimated by density of the bands on X-ray films relative to a standard curve generated with recombinant enzymes.

Competitive Activation of [^{3}H]-BP-7,8-diol by AKR1A1 and P4501B1 in Cell Culture Models. The following cells, (AKR1A1$^-$/P4501B1$^-$), (AKR1A1$^+$/P4501B1$^-$), (AKR1A1$^-$/P4501B1$^+$), and (AKR1A1$^+$/P4501B1$^+$), were treated with 4 μM [^{3}H]-BP-7,8-diol (5×10^5 cpm/nmol, final 0.5% DMSO in culture media) in 2 mL HBSS buffer containing 400 μM β-cyclodextrin as PAH carrier. Before harvesting the cells, 0.5 nmol BP-4,5-diol was added to cell culture dishes as internal standard to normalize for losses in the sample workup and analysis. The total cell culture mixture was harvested by a cell scraper into a 10-mL test tube and extracted twice with 3 mL water-saturated ethyl acetate. The organic extract and aqueous extract were isolated and analyzed by scintillation counting. The organic extract obtained after centrifugation at 2000*g* for 10 min was dried under vacuo. The residue was redissolved in 150 μL methanol, and a 40-μL aliquot was subjected to chromatographic analysis. Quantitation of [^{3}H]-BP-7,8-dione and [^{3}H]-BP-tetrols generated in the cells was accomplished using a tandem Waters Alliance 2695 chromatographic system (Waters Corp., Milford, MA) with a Waters 996 photodiode array detector and a β-RAM in-line radioactive detector (IN/US Systems, Inc., Tampa, FL) as previously published (*40*). The quantity of the metabolites was determined by using the specific radioactivity of [^{3}H]-BP-7,8-diol (5×10^5 cpm/nmol) as conversion factor.

Identification of BP-7,8-diol Metabolites in Cellular Culture by HPLC/MS. The cells (~2×10^7) were treated with nonradiolabeled BP-7,8-diol (final 4 μM) in the media as described above for 12 h. After the culture mixture was extracted with ethyl acetate and the organic extract was dried under vacuo, the residue was redissolved in 150 μL methanol, and a 40-μL aliquot was subjected to LC/MS analysis. Mass spectrometric data were acquired using a Finnigan LCQ ion trap mass spectrometer (ThermoQuest, San Jose, CA) equipped with a Finnigan electrospray ionization (ESI) source. The mass spectrometer was operated in the positive ion mode. On-line chromatography was performed using a Waters Alliance 2690 HPLC system (Waters Corp., Milford, MA). A reversed-phased column (Zorbax-ODS C18, 5 μm, 4.6 mm × 250 mm, DuPont Co., Wilmington, DE) was used at a flow rate of 0.5 mL/min. Solvent A was 5 mM ammonium acetate in water containing 0.02% formic acid, and solvent B was 5 mM ammonium acetate in methanol containing 0.02% formic acid. The column was developed under a linear gradient [55−70% methanol (v/v) over 20 min, 70−80% methanol (v/v) for 10 min, and 80% methanol (v/v) for 20 min]. The eluant on-line was monitored for UV absorbance at 254 nm and by the mass spectrometer using the specific ion selection channels of BP-7,8-diol (*m*/*z* 268.5−269.5), BP-7,8-dione (*m*/*z* 282.5−283.5), and BP-tetrols (*m*/*z* 302.5−303.5) as well as a product ion scan. Identification of the metabolite peaks was achieved by comparing chromatographic retention times (RT), UV spectra, and MS spectra of the metabolites with those obtained for the authentic standards.

Induction of P4501B1 by Either BP-7,8-dione or BP-7,8-diol Activated by AKR1A1. The parental H358 cells (AKR1A1$^-$/P4501B1$^-$) were treated with BP-7,8-dione at the concentration of 0, 0.01, 0.1, 1, and 10 μM for 12 h. The dose response of BP-7,8-dione on P4501B1 mRNA levels was determined by Northern blotting. To establish the time course, H358 cells were treated with BP-7,8-dione (4 μM) for 0, 1, 3, 6, and 12 h and analyzed for P4501B1 induction. In the AKR1A1-transfected cells (AKR1A1$^+$/P4501B1$^-$), the dose response to BP-7,8-diol was monitored using concentrations of 0, 0.01, 1, 10, and 20 μM for 12 h, and the time course was performed over 0, 1, 3, 6, and 12 h using 4 μM BP-7,8-diol and P4501B1 mRNA levels measured. The parental cells were used as a control group. Induction of P4501B1 protein by either BP-7,8-dione or AKR1A1 transfectants treated with BP-7,8-diol was measured in a similar manner using Western blot analysis as described earlier.

Pharmacological Manipulation of P4501B1 Induction. The AKR1A1$^-$/P4501B1$^-$ and AKR1A1$^+$/P4501B1$^-$ cells were co-treated with 4 μM PAH [(±)*anti*-BPDE, (±)-BP-7,8-diol, or BP-7,8-dione] and various inhibitors [SNM (50 μM), NAC (5 mM), and DFB (1μM)] for 12 h following earlier pretreatments with the inhibitors for 12 h. P4501B1 mRNA levels were analyzed by Northern blotting. To measure metabolic profiles, cells were pretreated with the inhibitors [SNM, NAC, DFB, and TMS] for 12 h and then co-treated with [^{3}H]-(±)-BP-7,8-diol for a subsequent 12 h. The cell culture mixture was processed as described above. After extraction with ethyl acetate, the organic extracts were dried under vacuo, and the residue was redissolved with methanol and subjected to HPLC/UV/β-RAM analysis. The amount of [^{3}H]-BP-tetrols generated in the cells was determined by the specific radioactivity (5×10^5 cpm/nmol) of [^{3}H]-(±)-BP-7,8-diol.

Results

Coexpression of AKR1A1 and P4501B1 in H358 Cell Culture Models. H358 bronchoalveolar cells (AKR1A1 null, P4501A1/P4501B1 null) were manipulated to express either one or both enzyme systems, Figure 2A. Expression of P4501B1 mRNA was approximately 20-fold higher than P4501A1 mRNA in the cells treated with TCDD. AKR1A1 stable transfectants showed a high expression of AKR1A1 transcripts. Coexpression of P4501B1 and AKR1A1 was obtained after AKR1A1-transfected cells were treated with TCDD. Thus, the following

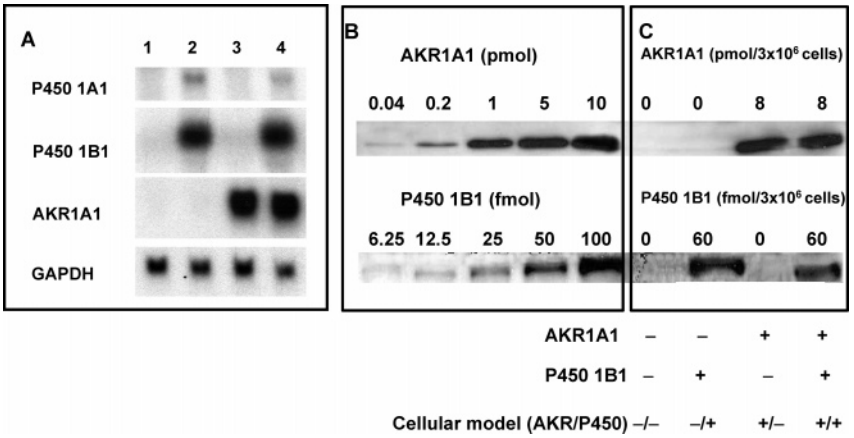

Figure 2. Phenotypes of human bronchoalveolar cells that coexpress AKR1A1 and P4501B1. Parental H358 cells were stably transfected with AKR1A1-cDNA and both cell types were induced by TCDD (10 nM for 12 h) for P4501B1 induction. (A) The expression of AKR1A1, P4501A1, and P4501B1 transcripts in the cellular models by Northern blotting analysis. RNA (20 μg) from AKR1A1$^-$/P4501B1$^-$ cells (lane 1), AKR1A1$^-$/P4501B1$^+$ cells (lane 2), AKR1A1$^+$/P4501B1$^-$ cells (lane 3), and AKR1A1$^+$/P4501B1$^+$ cells (lane 4) was applied to a 1% agarose/formaldehyde gel. Following electrophoresis, the transfer membrane was probed for the expression of the transcript indicated (see Materials and Methods). GAPDH probe was used as a control to standardize for the transfer and loading of the RNA. (B) Standards for quantitation of AKR1A1 and P4501B1 protein by immunoblot analysis. Recombinant AKR1A1 (range, 0.04−10 pmol) or P4501B1 (range, 6.25−100 fmol) were separated by SDS−PAGE, electrotransferred to nitrocellulose membranes, and blotted with either polyclonal rabbit anti-human AKR1A1 antiserum (1:2000 dilution) or rabbit anti-human P4501B1 antiserum (1:2000 dilution). The immunoblots were developed by incubation with the goat anti-rabbit IgG−horseradish peroxidase conjugate as secondary antibody followed by ECL detection. (C) Quantitation of the levels of AKR1A1 and P4501B1 in the cellular models. The amount of AKR1A1 and P4501B1 in cell lysates (60 μg total protein) was estimated by comparing their relative density to known amounts of recombinant enzymes. The estimated amounts are shown above the top of each lane.

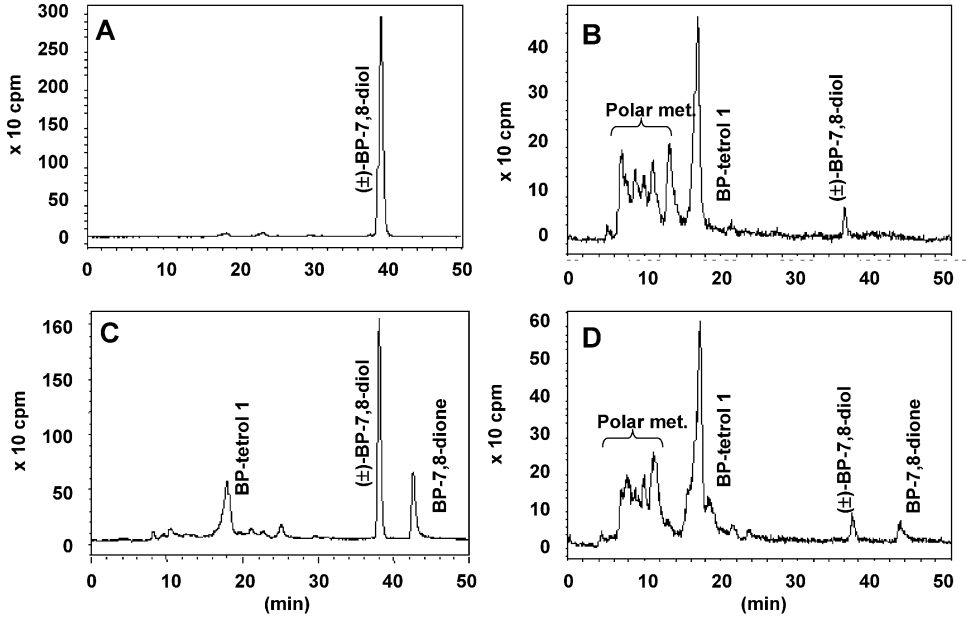

Figure 3. Metabolic profiles of BP-7,8-diol in the cell culture models. The cells ($\sim 2 \times 10^7$) were incubated with [^{3}H]-(±)-BP-7,8-diol (4 μM, 5 $\times$ 10^5 cpm/nmol) for the time indicated, and the mixture was extracted with ethyl acetate. The organic extracts were dried and redissolved in methanol for HPLC/UV/β-RAM analysis. The analytical conditions was described in Materials and Methods. (A) Parental cells; (B) AKR1A1$^-$/P4501B1$^+$ cells; (C) AKR1A1$^+$/P4501B1$^-$ cells; and (D) AKR1A1$^+$/P4501B1$^+$ cells. (A−C) The chromatograms after 12 h of treatment; (D) the chromatogram after 6 h of treatment.

cell lines were available: AKR1A1$^-$/P4501B1$^-$, AKR1A1$^+$/P4501B1$^-$, AKR1A1$^-$/P4501B1$^+$, and AKR1A1$^+$/P4501B1$^+$. To compare the protein levels of AKR1A1 and P4501B1 in these cellular models, quantitative immunoblot assays were performed, Figure 2B,C. The amount of AKR1A1 protein expressed in AKR1A1$^+$ cells was in the range of 8 pmol/3 $\times$ 10^6 cells, and the amount of membrane-bound P4501B1 was in the range of 60 fmol/3 $\times$ 10^6 cells. Thus, the amount of cytosolic AKR1A1 appeared to be 100 times more abundant than the membrane-bound P4501B1.

Metabolic Profiling of [^{3}H]-BP-7,8-diol in the Intact H358 Cells. The metabolic profiles of [^{3}H]-BP-7,8-diol in the cell culture models were examined using HPLC/UV/β-RAM detection, Figure 3A−D. In the control cells (AKR1A1$^-$/P4501B1$^-$), a radiochromatogram of the organic extracts showed that no significant BP-7,8-diol metabolism occurred. However, [^{3}H]-BP-7,8-diol was converted to the *anti*-BPDE hydrolysis product BP-tetrol-1 in AKR1A1$^-$/P4501B1$^+$ cells. In addition, chromatographic peaks eluted ahead of the BP-tetrol-1 peak, indicating the potential for *anti*-BPDE to form metabolites of increased polarity. In AKR1A1$^+$/P4501B1$^-$ cells, [^{3}H]-BP-7,8-diol was activated to BP-7,8-dione. Unexpectedly, [^{3}H]-BP-tetrols were also detected, even though these cells do not constitutively express P4501B1, indicating that P4501B1 induc-

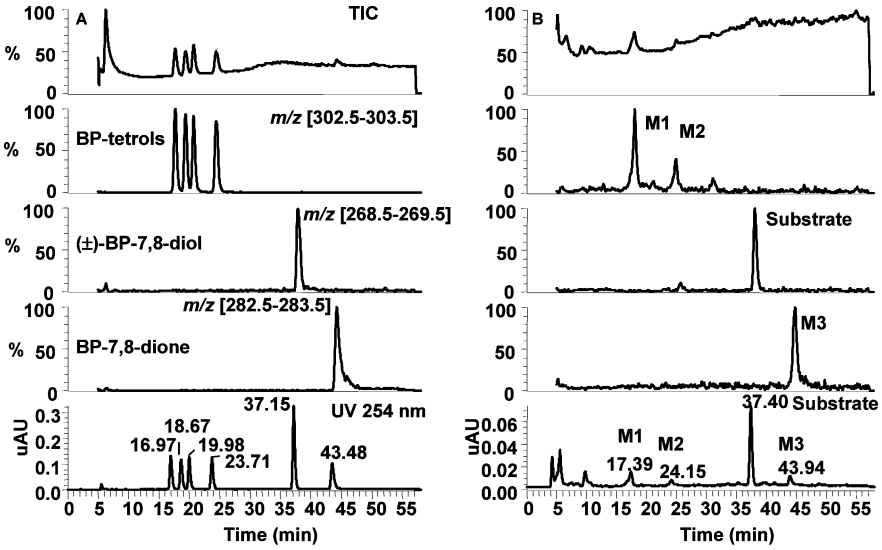

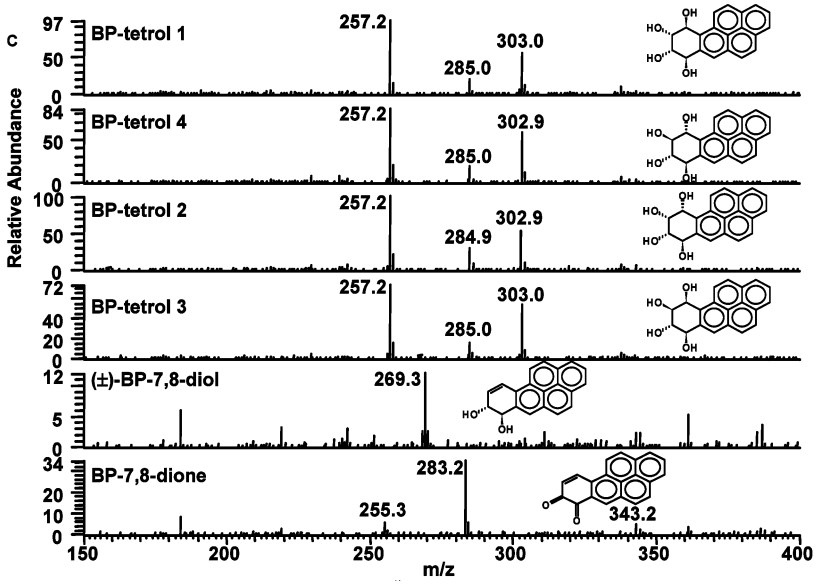

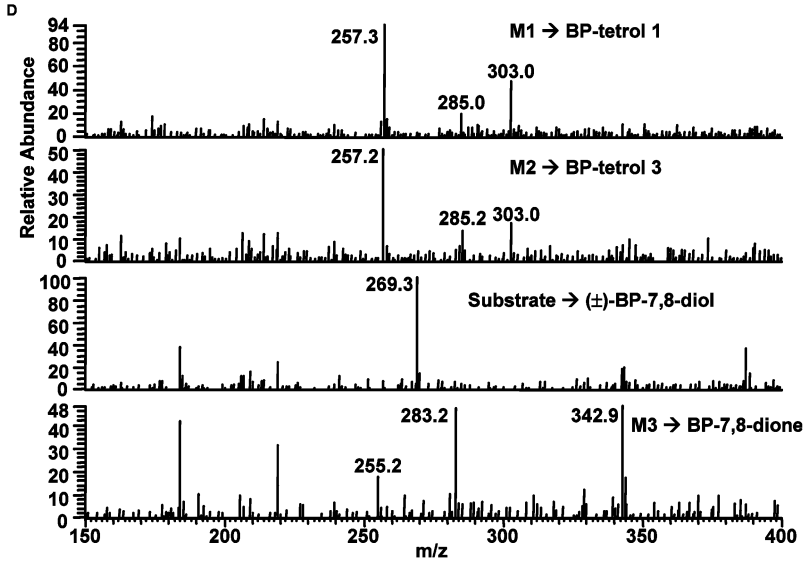

Figure 4. (Continued)

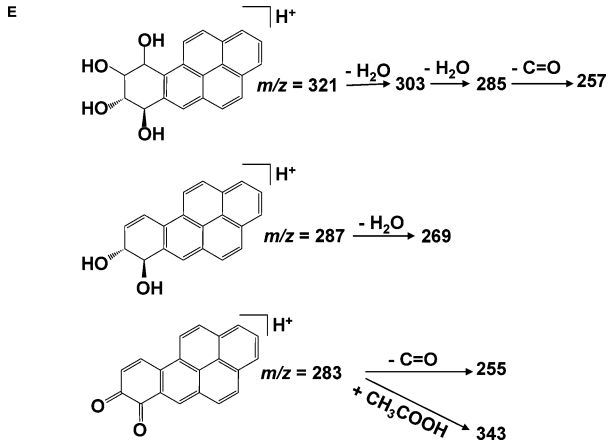

Figure 4. Identification of BP-7,8-diol metabolites in human bronchoalveolar cells by LC/MS. The AKR1A1$^+$/P4501B1$^-$ cells ($\sim 2 \times 10^7$) were treated with unlabeled (±)-BP-7,8-diol (4 μM) for 12 h, and the total culture mixture was extracted with ethyl acetate. The organic extracts were dried and redissolved in methanol for LC/MS analysis. Chromatographic and mass spectrum data were obtained following separation on an ODS column using on-line monitoring of metabolites at UV 254 nm and specific positive ion selection channels of BP-7,8-diol (*m*/*z* 268.5−269.5), BP-7,8-dione (*m*/*z* 282.5−283.5), and BP-tetrols (*m*/*z* 302.5−303.5). MS/MS spectra were obtained by using the Dependent Product Ion Scan mode for detection. (A) Chromatographic characteristics of authentic standards. (B) Chromatographic characteristics of unknown metabolites in the cells. M1 = BP-tetrol-1, RT = 17.39 min; M2 = BP-tetrol-3, RT = 24.15 min; M3 = BP-7,8-dione, RT = 43.94 min; Substrate = BP-7,8-diol, RT = 37.40 min. (C) MS/MS spectra of the authentic standards. (D) MS/MS spectra of the BP-7,8-diol metabolites produced in the cells. (E) Proposed fragmentation patterns for BP-tetrols, BP-7,8-diol, and BP-7,8-dione. The losses of 18 amu (H_2O) and 28 amu (C═O) were the main pathways for the generation of product ions.

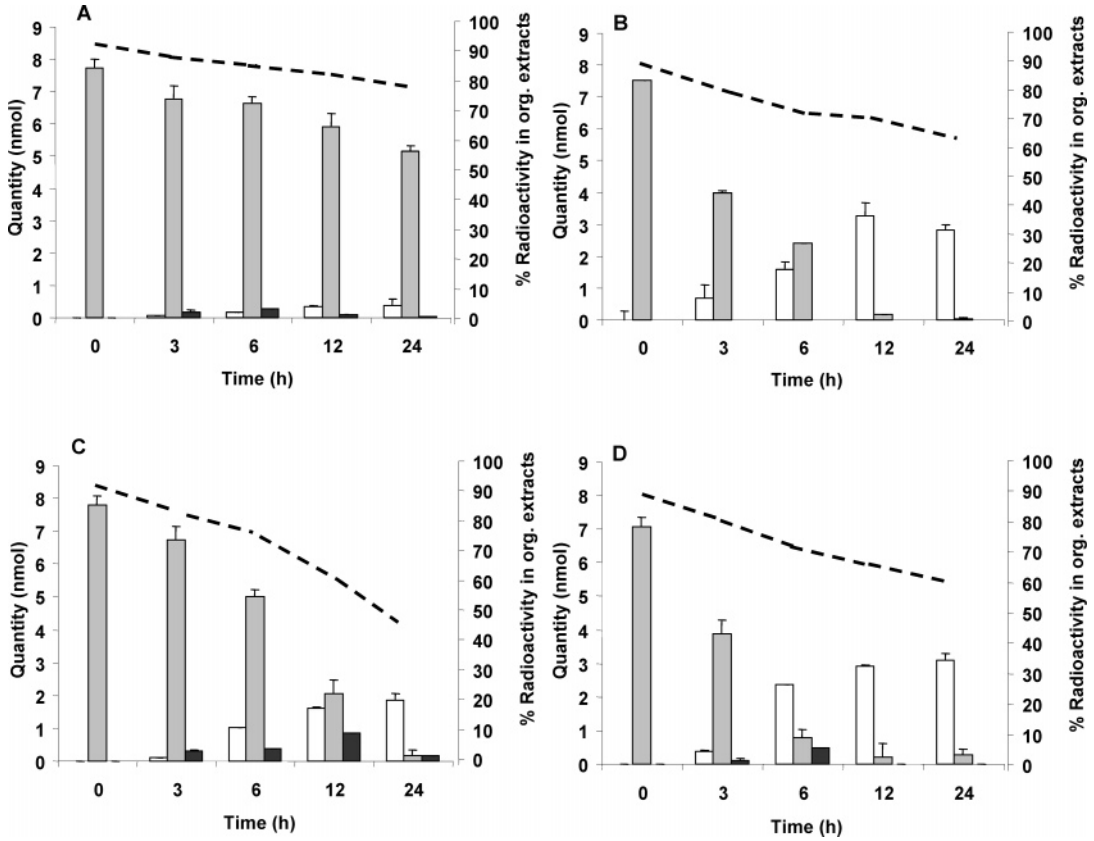

Figure 5. Quantitation of the competing roles of AKR1A1 and P4501B1 in the activation of (±)-BP-7,8-diol in the cellular models. The cellular models were treated with [^{3}H]-(±)-BP-7,8-diol (4 μM, 500 000 cpm/nmol) for 0, 3, 6, 12, and 24 h. After culture, the mixture was extracted, the organic extract was dried and redissolved in methanol, and an aliquot was analyzed by HPLC/UV/β-RAM. Radioactive peaks in the chromatograms were integrated and normalized to amount (nmol) using the specific radioactivity of the isotope. (A) AKR1A1$^-$/P4501B1$^-$ cells; (B) AKR1A1$^-$/P4501B1$^+$ cells; (C) AKR1A1$^+$/P4501B1$^-$ cells; (D) AKR1A1$^+$/P4501B1$^+$ cells. Empty box, BP-tetrol-1; gray box, BP-7,8-diol; black box, BP-7,8-dione; ---, %distribution of radioactivity in the organic extracts.

tion had occurred. In AKR1A1$^+$/P4501B1$^+$ cells, [^{3}H]-BP-7,8-diol was converted to both BP-7,8-dione and BP-tetrol-1 due to the coexpression of AKR1A1 and P4501B1 in the cells.

Identification of BP-7,8-diol Metabolites in H358 Cells by HPLC/MS. To validate the identity of the BP-7,8-diol metabolites, metabolic profiling was replicated in the cellular models using unlabeled material. Organic extracts were analyzed by HPLC/MS, Figure 4. Metabolites were identified relative to authentic synthetic standard compounds, BP-tetrols (MH^+ = *m*/*z* 303, $RT_{tetrol-1}$ = 16.97, $RT_{tetrol-2}$ = 19.98, $RT_{tetrol-3}$ = 23.71, $RT_{tetrol-4}$ = 18.67), BP-7,8-diol (MH^+ = *m*/*z* 269, RT = 37.15) and BP-7,8-dione (MH^+ = *m*/*z* 283, RT = 43.48),

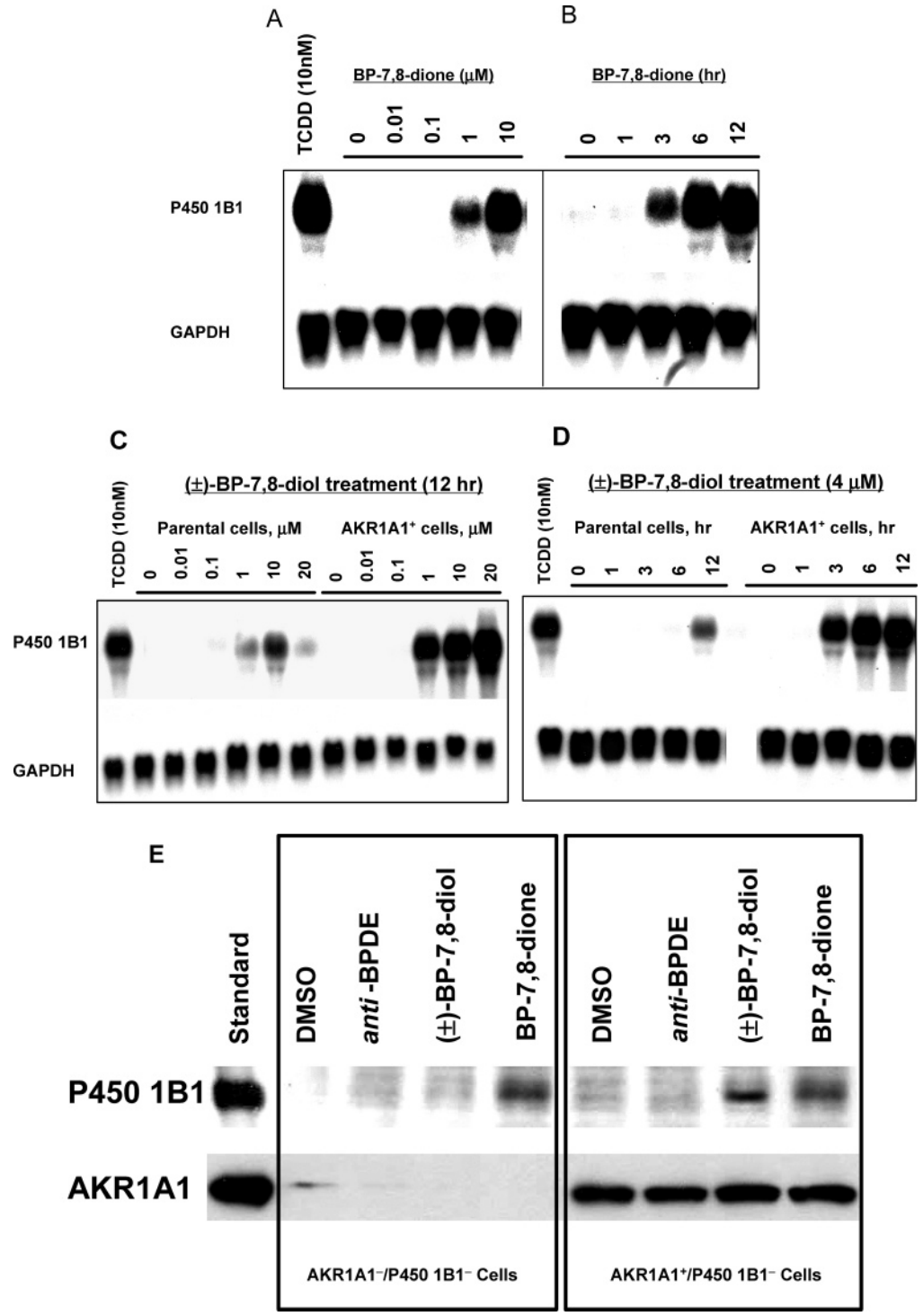

Figure 6. Induction of P4501B1 in parental and AKR1A1-transfected cells by BP-7,8-dione or by BP-7,8-diol. Parental H358 cells and AKR1A1 transfectants were treated with BP-7,8-dione or (±)-BP-7,8-diol as indicated and subjected to Northern (A−D) and Western blot analysis (E). Induction of P4501B1 in parental cells by BP-7,8-dione showed concentration (A) and time (B) dependence. Induction of P4501B1 by BP-7,8-diol in parental and AKR1A1 transfectants showed concentration (C) and time (D) dependence. Induction of P4501B1 protein by *anti*-BPDE, BP-7,8-diol, and BP-7,8-dione in parental cells (AKR1A1$^-$/P4501B1$^-$) and AKR1A1 transfectants (AKR1A1$^+$/P4501B1$^-$ cells) measured by Western blot analysis. Cells were treated with 20 μM inducer over 12 h, and 60 μg of cellular protein was applied to each lane of the gel (E).

Figure 4A,C. The formation of BP-tetrol-1 (M1, $MH^+ = m/z$ 303, RT = 17.39 min), BP-tetrol-3 (M2, $MH^+ = m/z$ 303, RT = 24.15 min), and BP-7,8-dione (M3, $MH^+ = m/z$ 283, RT = 43.94 min) in the cells were confirmed by the total ion chromatograms in the channel of m/z [302.5−303.5], m/z [302.5−303.5], and [282.5−283.5], respectively, Figure 4B,D. The corresponding product ion spectra were also collected for the identification of fragment ions. The prominent product ions observed were m/z 257.2, 285.0, and 303.0 for BP-tetrols ($MH^+ = m/z$ 321), m/z 269 for BP-7,8-diol ($MH^+ = m/z$ 287), and m/z 283 for BP-7,8-dione ($MH^+ = m/z$ 283). The ion m/z 343.2 corresponds to an ion for the BP-7,8-dione−CH_3COOH adduct. The fragmentation patterns of the metabolites (BP-7,8-dione and BP-tetrols) were almost identical to the authentic standards, which verified the generation of BP-7,8-dione and BP-tetrols in the cells by comparing Figure 4C,D. The proposed MS^2 fragmentation patterns of the metabolites were interpreted by

the loss of 18 amu for H_2O and the loss of 28 amu for C═O, Figure 4E.

Quantitation of BP-7,8-diol Metabolites over Time in the H358 Cell Models. The quantities of PAH metabolites formed over time were estimated using the specific radioactivity of the substrate [^{3}H]-BP-7,8-diol once the chromatographic peaks of the metabolites were integrated, Figure 5. The distribution of radioactivity in the organic extracts was significantly decreased over time due to the appearance of polar metabolites that were detected as radioactivity in the aqueous phase. [^{3}H]-BP-tetrols increased over 3−12 h to a constant level in AKR1A1$^-$/P4501B1$^+$ cells, Figure 5B. In contrast, formation of [^{3}H]-BP-7,8-dione was initially elevated for 3−12 h and significantly decreased after 24 h in AKR1A1$^+$/P4501B1$^-$ cells, showing that generation of BP-7,8-dione was a transient event followed by secondary metabolism. Unexpectedly, formation of BP-tetrol-1 was observed after BP-7,8-dione generation in the AKR1A1$^+$/P4501B1$^-$ cells, Figure 5C. In cells expressing both pathways (AKR1A1$^+$/P4501B1$^+$), the generation of [^{3}H]-BP-tetrols was slightly elevated over that seen in the AKR1A1$^-$/P4501B1$^+$ cells, while the levels of [^{3}H]-BP-7,8-dione decreased rapidly after 6 h, Figure 5D. The results implied that, in addition to AKR1A1 and P4501B1 competing for BP-7,8-diol activation, the formation of BP-tetrol-1 in the AKR1A1$^+$/P4501B1$^-$ cells was temporally related to BP-7,8-dione formation, suggesting that BP-7,8-dione induced P4501B1.

Induction of P4501B1 by AKR1A1-Downstream Metabolite BP-7,8-dione. To confirm the hypothesis that AKR1A1 induces P4501B1 expression via formation of BP-7,8-dione, which then acts as a ligand for the AhR, induction experiments were performed. In the positive control, BP-7,8-dione was found to be an inducer of P4501B1 in AKR1A1$^-$/P4501B1$^-$ cells in a dose- and time-dependent manner, Figure 6A,B. In AKR1A1$^+$/P4501B1$^-$ cells treated with BP-7,8-diol, induction of P4501B1 was again observed in a dose- and time-dependent manner. In the parental AKR1A1$^-$/P4501B1$^-$ cells, BP-7,8-diol was significantly less effective as an inducer of P4501B1, Figure 6C,D. Western blot analysis further confirmed that BP-7,8-diol only functioned as a P4501B1 inducer when AKR1A1 was expressed, Figure 6E. In contrast, *anti*-BPDE had no effect on the induction of P4501B1.

Pharmacological Manipulation of P4501B1 Induction. To confirm that P4501B1 induction by BP-7,8-diol in AKR1A1$^+$/P4501B1$^-$ cells requires AKR1A1 activity and the transactivation of P4501B1 gene via the AhR/Arnt (AhR-nuclear translocator)/XRE signaling pathway, the cells were manipulated pharmacologically. The effects of the AKR1A1 inhibitor (SNM), the *o*-quinone scavenger (NAC), and AhR antagonist (DFB) on the induction of P4501B1 were determined by Northern blotting analysis. The results showed that SNM, NAC, and DFB completely blocked P4501B1 induction by BP-7,8-diol, Figure 7A. When the formation of BP-tetrols was monitored following these treatments, it was found that BP-tetrol levels fell consistent with this model. SNM, NAC, DFB, and TMS all reduced BP-tetrol levels, where TMS acts as a competitive inhibitor of P4501B1 activity, Figure 7B.

Discussion

This study compares the activation of BP-7,8-diol by AKR and P4501B1 pathways in human lung bronchoalveolar cells. The products (BP-7,8-dione and BP-tetrols) formed via AKR1A1 and P4501B1 in the cell culture models were identified by LC/MS and quantitatively measured by HPLC coupled with in-line radioactive detection (HPLC/UV/β-RAM) using [^{3}H]-(±)-BP-7,8-diol as tracer. Generation of BP-7,8-dione by AKR1A1 and BP-tetrols by P4501B1 in the cellular models confirmed the competing roles of AKR1A1 and P4501B1 in BP-7,8-diol activation. Transient generation of BP-7,8-dione in AKR1A1$^+$/P4501B1$^-$ cells resulted in the formation of the *anti*-BPDE hydrolysis product BP-tetrol due to the subsequent induction of P4501B1. Northern and Western blot analysis further confirmed that BP-7,8-dione or BP-7,8-diol activated by AKR1A1 induced P4501B1 expression. Pharmacological manipulation of the AhR/Arnt/XRE pathway confirmed that the mechanism of induction of P4501B1 by the AKR1A1 metabolite BP-7,8-dione occurred via the AhR receptor.

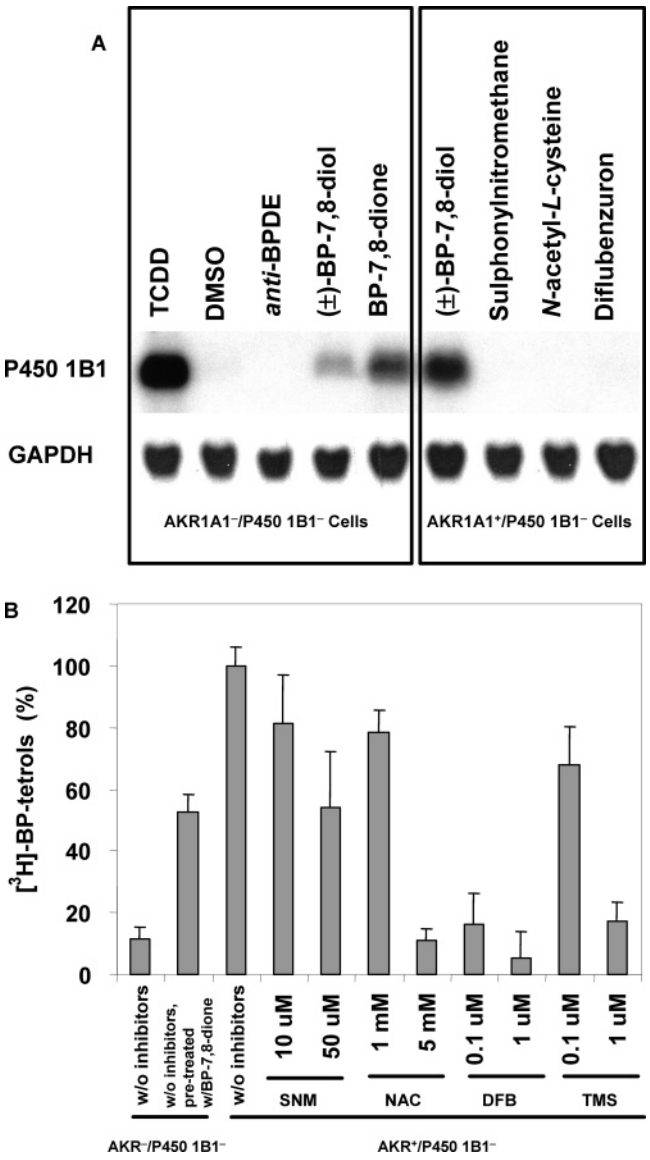

Figure 7. Attenuation of P4501B1 induction by pharmacological agents. (A) Parental cells (AKR1A1$^-$/P4501B1$^-$) were treated with 20 μM of *anti*-BPDE, BP-7,8-diol, and BP-7,8-dione for 12 h, respectively, and P4501B1 induction was measured by Northern analysis, left panel; transfected cells (AKR1A1$^+$/P4501B1$^-$) were induced with 4 μM BP-7,8-diol for 12 h, and the ability of 50 μM sulfonylnitromethane (SNM, an AKR1A1 inhibitor), 5 mM *N*-acetyl-L-cysteine (NAC, an *o*-quinone scavenger), and 1 μM diflubenzuron (DFB, an AhR antagonist) to block P4501B1 induction was monitored by Northern analysis,right panel. (B) Attenuation of BP-tetrol formation in transfected cells treated with 4 μM BP-7,8-diol in the presence and absence of SNM, NAC, DFB, and tetramethoxy stilbene (TMS, a P4501B1 inhibitor). BP-tetrol formation was analyzed by HPLC/UV/β-RAM, panel B. As a positive control, formation of BP-tetrols in parental cells pre-treated with 20 μM BP-7,8-dione is shown.

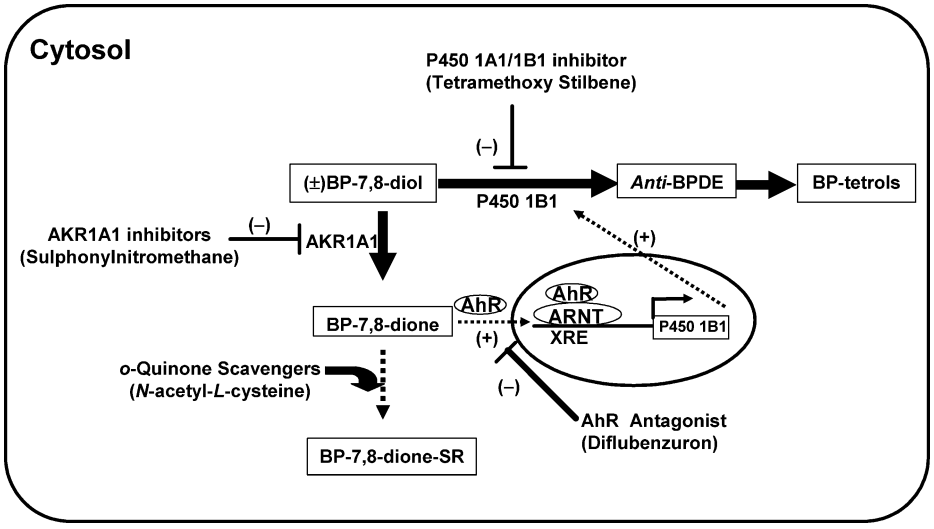

Figure 8. Induction of P4501B1 by the AKR pathway and its pharmacological manipulation.

Among AKRs, AKR1A1 or aldehyde reductase was the focus of this study because an in vitro comparison of the five human AKRs (AKR1A1 and AKR1C1−AKR1C4) implicated in PAH *trans*-dihydrodiol oxidation showed that this general metabolic enzyme was the most efficient in oxidizing BP-7,8-diol (*39*, *41*). Moreover, AKR1A1 was stereoselective in that it oxidized only the (−)-BP-7,8-diol, which is the relevant stereoisomer produced metabolically (*41*). Other PAH *trans*-dihydrodiols oxidized by AKR1A1 include the non-K region *trans*-dihydrodiols of chrysene, 5-methylchrysene, benz[*a*]anthracene (BA), and 7,12-dimethylbenz[*a*]anthracene (DMBA). Methylation increased catalytic efficiency significantly for AKR1A1 and the human AKR1C isoforms (*39*−*41*). The result of human multiple tissue expression arrays showed that P4501A1/P4501B1/AKR1A1/EH are coexpressed in sites of PAH activation (*39*). The high catalytic efficiency of AKR1A1 for potent proximate carcinogen *trans*-dihydrodiols and its coexistence with P4501B1 and EH suggest that it plays an important role in this alternative pathway of PAH activation.

P4501A1 and P4501B1 are the key metabolic enzymes involved in PAH metabolism and are inducible via transactivation by AhR ligands such as planar aromatics, 3-methylcholanthrene, β-naphthoflavone, and various PAH (*42*−*45*). When TCDD was used as a P4501B1 inducer, it was found that P4501B1 induction was at least 10 times favored over P4501A1 in H358 cells. By contrast, in human hepatoma cells (HepG2), the induction of P4501A1 was observed in the absence of P4501B1 expression, indicating that induction of P4501A1 and P4501B1 via AhR ligands is tissue-specific (*46*, *47*). Such differential induction of P4501A1 and P4501B1 in HepG2 cells and H358 cells, respectively, by TCDD provides a model to discriminate the relative role of either P4501A1 or P4501B1 in PAH activation.

Coexpression of AKR1A1 and P4501B1 and functional activation of BP-7,8-diol were previously documented in cell extracts of human bronchoalveolar H358 cellular models (*40*). In this study, generation of BP-7,8-diol metabolites (BP-7,8-dione and BP-tetrols) in the intact cells was verified by HPLC/UV/MS. The formation of BP-7,8-dione in the AKR1A1 transfected cells provided a cellular readout of the AKR pathway. We also observed the interplay between the AKR1A1 and P4501B1 pathways of BP-7,8-diol activation; that is, activation of BP-7,8-diol to BP-7,8-dione by AKR1A1 and elevated *anti*-BPDE formation due to the P4501B1 induction. This induction provided an unexpected cellular readout of the AKR pathway of PAH activation that was even more prominent than BP-7,8-dione formation.

Previously, it was shown that BP-7,8-dione acts as AhR agonist and induces P4501A1 expression in HepG2 cells by binding to the AhR, which translocates to the nucleus and activates P4501A1 gene transcription via a xenobiotic response element (XRE) (*46*). Although the AhR demonstrates a strict specificity for planar aromatics, nonplanar BP-7,8-diol also induced P4501A1 expression in HepG2 cells over a delayed time course due to its metabolic activation to BP-7,8-dione. BP-7,8-dione was a more potent inducer of P4501A1 when compared with the 1,6-, 3,6-, and 6,12-benzo[*a*]pyrenediones. HepG2-101L cells stably transfected with a XRE−luciferase construct showed that BP-7,8-dione activated P4501A1 transcription via a XRE-dependent mechanism. BP-7,8-dione failed to induce P4501A1 in AhR-deficient and Arnt-deficient murine hepatoma cell lines and confirmed that induction of P4501A1 was AhR- and -dependent. Electrophoretic mobility shift assays demonstrated the specific appearance of a BP-7,8-dione-activated AhR complex in the nucleus, and immunofluorescence studies confirmed that BP-7,8-dione mediated nuclear translocation of the AhR. These observations may provide an explanation for the work of Tukey et al. who implied that BP-7,8-diol was an inducer of P4501A1 in HepG2 cells (*47*). This present study now shows that this mechanism of induction operates in human lung cells and requires AKR1A1 expression. P4501B1 induction was attenuated by an AKR1A1 inhibitor (SNM), by an *o*-quinone scavenger (NAC), and by an AhR antagonist (DFB). A functional consequence of this induction was a re-direction of PAH metabolism which resulted in elevated BP-tetrol formation. This elevated BP-tetrol formation was blocked by the P4501B1 inhibitor TMS, Figure 8. An alternative explanation for the NAC response could be the removal of reactive oxygen species. However, we do not believe this to be the case. NAC forms mercapturic acid conjugates with BP-7,8-dione (*48*), and this change in planarity of structure likely eliminates binding to the AhR. Moreover, in unpublished results, we find that the NAC−quinone conjugate redox-cycles better than the parent quinone (Penning, unpublished). If ROS were the P4501B1 inducer, formation of the mercapturic acid conjugate should increase P4501B1 expression. The functional interplay between the AKR and P450 pathways indicates that the role of AKR1A1 in the activation of BP-7,8-diol is bifunctional; that is, it directly activates BP-7,8-diol to the

reactive and redox-active PAH *o*-quinone (BP-7,8-dione); and it indirectly trans-activates the *P4501B1* gene by generating the AhR ligand BP-7,8-dione.

Planar non-K-region PAH *o*-quinones such as BP-7,8-dione are ligands for the AhR and also bind to the ryanodine receptor (*49*), the phorbol-ester receptor, and PKC (protein kinase C) (*50*). Submicromolar concentrations of BP-7,8-dione selectively modulate microsomal Ca^{2+} transport at the level of the SERCA-1 transporter, the ryanodine receptor. The effect was biphasic; there was an immediate activation of the receptor and a subsequent inactivation phase. The ryanodine receptor is known to have reactive cysteines which may be redox sensors. We postulate that the activation event is the result of ROS modification of the cysteines. By contrast, the inactivation of the receptor may occur due to arylation of the receptor by 1,4-Michael addition to the *o*-quinone. This effect was not seen with BP-1,6-dione, BP-3,6-dione or BP-6,12-dione, BP-7,8-diol, or *anti*-BPDE. Since the ryanodine receptor is broadly expressed in mammalian cells and intracellular Ca^{2+} is a known activator of cPKC isozymes (α, $\beta1$, $\beta2$, γ), PAH *o*-quinones may stimulate signal transduction pathways via these Ca^{2+} transients. Our results on the ryanodine receptor provide an important paradigm for the effects of PAH *o*-quinones on proteins with redox-sensitive cysteines, including the mitogen activated protein kinase (MAPK), fos, and jun. It is noteworthy that BP-7,8-diol fails to activate MAP kinase p38 or stimulate apoptosis in Arnt-deficient cells (*47*). It is possible that BP-7,8-diol initiates these events by metabolism to BP-7,8-dione rather than by metabolism to *anti*-BPDE. These receptor-mediated effects may also be biphasic, since the quinones are both redox-active and electrophilic.

PAH *o*-quinones, NP-1,2-dione, BP-7,8-dione, and DMBA-3,4-dione also inhibit both basal and stimulated recombinant PKCα (EC_{50} = 3.0 μM), and this effect is mediated via irreversible inhibition of the catalytic fragment. This effect is seen in the absence of redox-cycling conditions and is attributed to arylation of PKC by the *o*-quinone (*50*). This effect has been subsequently observed on PKCδ. The effect was not observed with the corresponding *trans*-dihydrodiols or diol epoxides and was therefore *o*-quinone-specific. Thus, generation of PAH *o*-quinones via AKRs may affect multiple signal transduction cascades (e.g., AhR and PKC) that could affect the initiation and promotion phases of lung carcinogenesis.

Acknowledgment. This study was supported by the NIH, Grant Nos. P01-CA92537 and R01-CA039504 (awarded to T.M.P.). We thank Mr. Yu-min Shen and Ms. Amy Quinn for technical assistance and helpful advice.

References

(1) Hecht, S. S. (1999) Tobacco smoke carcinogens and lung cancer. *J. Natl. Cancer Inst. 91*, 1194−1210.

(2) Cavalieri, E. L., and Rogan, E. G. (1995) Central role of radical cations in metabolic activation of polycyclic aromatic hydrocarbons. *Xenobiotica 25*, 677−688.

(3) Conney, A. H. (1982) Induction of microsomal enzymes by foreign chemicals and carcinogenesis by polycyclic aromatic hydrocarbons: G. H. A. Clowes Memorial Lecture. *Cancer Res. 42*, 4875−4917.

(4) Yang, S. K., McCourt, D. W., Roller, P. P., and Gelboin, H. V. (1976) Enzymatic conversion of benzo[*a*]pyrene leading predominantly to the diol-epoxide *r*-7,*t*-8-dihydroxy-*t*-9,10-oxy-7,8,9,10-tetrahydrobenzo-[*a*]pyrene through a single enantiomer of *r*-7,*t*-8-dihydroxy-7,8-dihydrobenzo[*a*]pyrene. *Proc. Natl. Acad. Sci. U.S.A. 73*, 2594−2598.

(5) Penning, T. M., Burczynski, M. E., Hung, C. F., McCoull, K. D., Palackal, N. T., and Tsuruda, L. S. (1999) Dihydrodiol dehydrogenases and polycyclic aromatic hydrocarbon activation: generation of reactive and redox active *o*-quinones. *Chem Res. Toxicol. 12*, 1−18.

(6) Nagao, M., and Sugimura, T. (1978) *Mutagenesis: Microbial Systems*, Vol. 1, pp 99−121, Academic Press, New York.

(7) Malaveille, C., Kuroki, T., Sims, P., Grover, P. L., and Bartsch, H. (1977) Mutagenicity of isomeric diol-epoxides of benzo[*a*]pyrene and benz[*a*]anthracene in S. typhimurium TA98 and TA100 and in V79 Chinese hamster cells. *Mutat. Res. 44*, 313−326.

(8) Newbold, R. F., and Brookes, P. (1976) Exceptional mutagenicity of a benzo[*a*]pyrene diol epoxide in cultured mammalian cells. *Nature 261*, 52−54.

(9) Buening, M. K., Wislocki, P. G., Levin, W., Yagi, H., Thakker D. R., Akagi H., Koreeda, M., Jerina, D. M., and Conney, A. H. (1978) Tumorigenicity of the optical enantiomers of the diastereomeric benzo-[*a*]pyrene 7,8-diol-9,10-epoxides in newborn mice: exceptional activity of (+)-7,8-dihydroxy-9,10-epoxy-7,8,9,10-tetrahydrobenzo[*a*]pyrene. *Proc. Natl. Acad. Sci. U.S.A. 75*, 5358−5361.

(10) Kapitulnik, J., Wislocki, P. G., Levin, W., Yagi, H., Jerina, D. M., and Conney, A. H. (1978) Tumorigenicity studies with diol-epoxides of benzo[*a*]pyrene which indicate that (+/−)-*trans*-7,8-dihydroxy-9,10-epoxy-7,8,9,10-tetrahydrobenzo[*a*]pyrene is an ultimate carcinogen in newborn mice. *Cancer Res. 38*, 354−358.

(11) Chang, R. L., Wood, A. W., Conney, A. H., Yagi, H., Sayer, J. M., Thakker, D. R., Jerina, D. M., and Levin, W. (1987) Role of diaxial versus diequatorial hydroxyl groups in the tumorigenic activity of a benzo[*a*]pyrene bay-region diol epoxide. *Proc. Natl. Acad. Sci. U.S.A. 84*, 8633−8636.

(12) Jeffrey, A. M., Jennette, K. W., Blobstein, S. H., Weinstein, I. B., Beland, F. A., Harvey, R. G., Kasal, H., Miura, I., and Nakanishi, K. (1976) Letter: Benzo[*a*]pyrene-nucleic acid derivative found in vivo: structure of a benzo[*a*]pyrenetetrahydrodiol epoxide-guanosine adduct. *J. Am. Chem. Soc. 98*, 5714−5715.

(13) Jerina, D. M., Chadha, A., Cheh, A. M., Schurdak, M. E., Wood, A. W., and Sayer, J. M. (1991) Covalent bonding of bay-region diol epoxides to nucleic acids. *Adv. Exp. Med. Biol. 283*, 533−553.

(14) Cheng, S. C., Hilton, B. D., Roman, J. M., and Dipple, A. (1989) DNA adducts from carcinogenic and noncarcinogenic enantiomers of benzo[*a*]pyrene dihydrodiol epoxide. *Chem. Res. Toxicol. 2*, 334−340.

(15) Marshall, C. J., Vousden, K. H., and Phillips, D. H. (1984) Activation of c-Ha-*ras*-1 proto-oncogene by in vitro modification with a chemical carcinogen, benzo[*a*]pyrene diol-epoxide. *Nature 310*, 586−589.

(16) Puisieux, A., Lim, S., Groopman, J., and Ozturk, M. (1991) Selective targeting of *p53* gene mutational hotspots in human cancers by etiologically defined carcinogens. *Cancer Res. 51*, 6185−6189.

(17) Denissenko, M. F., Pao, A., Tang, M., and Pfeifer, G. P. (1996) Preferential formation of benzo[*a*]pyrene adducts at lung cancer mutational hotspots in *p53*. *Science 274*, 430−432.

(18) Flowers-Geary, L., Harvey, R. G., and Penning, T. M. (1993) Cytotoxicity of polycyclic aromatic hydrocarbon *o*-quinones in rat and human hepatoma cells. *Chem. Res. Toxicol. 6*, 252−260.

(19) Shou, M., Harvey, R. G., and Penning, T. M. (1993) Reactivity of benzo[*a*]pyrene-7,8-dione with DNA. Evidence for the formation of deoxyguanosine adducts. *Carcinogenesis 14*, 475−482.

(20) McCoull, K. D., Rindgen, D., Blair, I. A., and Penning, T. M. (1999) Synthesis and characterization of polycyclic aromatic hydrocarbon *o*-quinone depurinating N7-guanine adducts. *Chem. Res. Toxicol. 12*, 237−246.

(21) Balu, N., Padgett, W. T., Lambert, G. R., Swank, A. E., Richard, A. M., and Nesnow, S. (2004) Identification and characterization of novel stable deoxyguanosine and deoxyadenosine adducts of benzo[*a*]pyrene-7,8-quinone from reactions at physiological pH. *Chem. Res. Toxicol. 17*, 827−838.

(22) Park, J. H., Gopishetty, S., Szewczuk, L. M., Troxel, A. B., Harvey, R. G., and Penning, T. M. (2005) Formation of 8-oxo-7,8-dihydro-2′-deoxyguanosine (8-oxo-dGuo) by PAH o-quinones: involvement of reactive oxygen species and copper(II)/copper(I) redox cycling. *Chem. Res. Toxicol. 18*, 1026−1037.

(23) Sagher, D., and Strauss, B. (1983) Insertion of nucleotides opposite apurinic/apyrimidinic sites in deoxyribonucleic acid during in vitro synthesis: uniqueness of adenine nucleotides. *Biochemistry 22*, 4518−4526.

(24) Gardner, H. W., and Hamberg, M. (1993) Oxygenation of (3Z)-nonenal to (2*E*)-4-hydroxy-2-nonenal in the broad bean (*Vicia faba* L.). *J. Biol. Chem. 268*, 6971−6977.

(25) Schneider, C., Porter, N. A., and Brash, A. R. (2004) Autoxidative transformation of chiral ω6 hydroxy linoleic and arachidonic acids to chiral 4-hydroxy-2*E*-nonenal. *Chem. Res. Toxicol. 17*, 937−941.

(26) Lee, S. H., and Blair, I. A. (2000) Characterization of 4-oxo-2-nonenal as a novel product of lipid peroxidation. *Chem. Res. Toxicol. 13*, 698−702.

(27) Sodum, R. S., and Chung, F. L. (1991) Stereoselective formation of in vitro nucleic acid adducts by 2,3-epoxy-4-hydroxynonanal. *Cancer Res. 51*, 137−143.

(28) Sodum, R. S., and Chung, F. L. (1989) Structural characterization of adducts formed in the reaction of 2,3-epoxy-4-hydroxynonanal with deoxyguanosine. *Chem. Res. Toxicol. 2*, 23−28.
(29) Lee, S. H., Arora, J. A., Oe, T., and Blair, I. A. (2005) 4-Hydroperoxy-2-nonenal-induced formation of 1,N^2-etheno-2′-deoxyguanosine adducts. *Chem. Res. Toxicol. 18*, 780−786.
(30) Rindgen, D., Nakajima, M., Wehrli, S., Xu, K., and Blair, I. A. (1999) Covalent modifications to 2′-deoxyguanosine by 4-oxo-2-nonenal, a novel product of lipid peroxidation. *Chem. Res. Toxicol. 12*, 1195−1204.
(31) Rindgen, D., Lee, S. H., Nakajima, M., and Blair, I. A. (2000) Formation of a substituted 1,N^6-etheno-2′-deoxyadenosine adduct by lipid hydroperoxide-mediated generation of 4-oxo-2-nonenal. *Chem. Res. Toxicol. 13*, 846−852.
(32) Lee, S. H., Rindgen, D., Bible, R. H., Jr, Hajdu, E., and Blair, I. A. (2000) Characterization of 2′-deoxyadenosine adducts derived from 4-oxo-2-nonenal, a novel product of lipid peroxidation. *Chem. Res. Toxicol. 13*, 565−574.
(33) Pollack, M., Oe, T., Lee, S. H., Silva Elipe, M. V., Arison, B. H., and Blair, I. A. (2003) Characterization of 2′-deoxycytidine adducts derived from 4-oxo-2-nonenal, a novel lipid peroxidation product. *Chem. Res. Toxicol. 16*, 893−900.
(34) Flowers, L., Ohnishi, S. T., and Penning, T. M. (1997) DNA strand scission by polycyclic aromatic hydrocarbon *o*-quinones: role of reactive oxygen species, Cu(II)/Cu(I) redox cycling, and *o*-semiquinone anion radicals. *Biochemistry 36*, 8640−8648.
(35) DeMarini, D. M., Brockman, H. E., de Serres, F. J., Evans, H. H., Stankowski, L. F., Jr., and Hsie, A. W. (1989) Specific-locus mutations induced in eukaryotes (especially mammalian cells) by radiation and chemicals: a perspective. *Mutat. Res. 220*, 11−29.
(36) Emerit, I., Keck, M., Levy, A., Feingold, J., and Michelson, A. M. (1982) Activated oxygen species at the origin of chromosome breakage and sister-chromatid exchanges. *Mutat. Res. 103*, 165−172.
(37) Cohen, S. M., and Ellwein, L. B. (1990) Cell proliferation in carcinogenesis. *Science 249*, 1007−1011.
(38) Cerutti, P. A. (1985) Prooxidant states and tumor promotion. *Science 227*, 375−381.
(39) Palackal, N. T., Burczynski, M. E., Harvey, R. G., and Penning, T. M. (2001) The ubiquitous aldehyde reductase (AKR1A1) oxidizes proximate carcinogen *trans*-dihydrodiols to *o*-quinones: potential role in polycyclic aromatic hydrocarbon activation. *Biochemistry 40*, 10901−10910.
(40) Jiang, H., Shen, Y. M., Quinn, A. M., and Penning, T. M. (2005) Competing roles of cytochrome P4501A1/1B1 and aldo-keto reductase 1A1 in the metabolic activation of (±)-7,8-dihydroxy-7,8-dihydrobenzo[*a*]pyrene in human bronchoalveolar cell extracts. *Chem. Res. Toxicol. 18*, 365−374.
(41) Palackal, N. T., Lee, S. H., Harvey, R. G., Blair, I. A., and Penning, T. M. (2002) Activation of polycyclic aromatic hydrocarbon *trans*-dihydrodiol proximate carcinogens by human aldo-keto reductase (AKR1C) enzymes and their functional overexpression in human lung carcinoma (A549) cells. *J. Biol. Chem. 277*, 24799−24808.
(42) Sutter, T. R., Tang, Y. M., Hayes, C. L., Wo, Y. Y., Jabs, E. W., Li, X., Yin, H., Cody, C. W., and Greenlee, W. F. (1994) Complete cDNA sequence of a human dioxin-inducible mRNA identifies a new gene subfamily of cytochrome P450 that maps to chromosome 2. *J. Biol. Chem. 269*, 13092−13099.
(43) Riddick, D. S., Huang, Y., Harper, P. A., and Okey, A. B. (1994) 2,3,7,8-Tetrachlorodibenzo-*p*-dioxin versus 3-methylcholanthrene: comparative studies of Ah receptor binding, transformation, and induction of CYP1A1. *J. Biol. Chem. 269*, 12118−12128.
(44) Khan, I. U., Bickers, D. R., Haqqi, T. M., and Mukhtar, H. (1992) Induction of CYP1A1 mRNA in rat epidermis and cultured human epidermal keratinocytes by benz[*a*]anthracene and β-naphthoflavone. *Drug Metab. Dispos. 20*, 620−624.
(45) Bowes, R. C., Parrish, A. R., Steinberg, M. A., Willett, K. L., Zhao, W., Savas, U., Jefcoate, C. R., Safe, S. H., and Ramos, K. S. (1996) Atypical cytochrome P450 induction profiles in glomerular mesangial cells at the mRNA and enzyme level. Evidence for CYP1A1 and CYP1B1 expression and their involvement in benzo[*a*]pyrene metabolism. *Biochem. Pharmacol. 52*, 587−5950
(46) Burczynski, M. E., and Penning, T. M. (2000) Genotoxic polycyclic aromatic hydrocarbon *ortho*-quinones generated by aldo-keto reductases induce CYP1A1 via nuclear translocation of the aryl hydrocarbon receptor. *Cancer Res. 60*, 908−915.
(47) Chen, S. C., Nguyen, N., Tamura, K., Karin, M., and Tukey, R. H. (2003) The role of the Ah receptor and p38 in benzo[*a*]pyrene-7,8-dihydrodiol and benzo[*a*]pyrene-7,8-dihydrodiol-9,10-epoxide-induced apoptosis. *J. Biol. Chem. 278*, 19526−19533.
(48) Murty, V. S., and Penning, T. M. (1992) Characterization of mercapturic acid and glutathionyl conjugates of benzo[*a*]pyrene-7,8-dione by two-dimensional NMR. *Bioconjugate Chem. 3*, 218−224.
(49) Pessah, I. N., Beltzner, C., Burchiel, S. W., Sridhar, G., Penning, T. M., and Feng, W. (2001) A reactive metabolite of benzo[*a*]pyrene, benzo[*a*]pyrene-7,8-dione, selectively alters microsomal Ca^{2+} transport and ryanodine receptor function. *Mol. Pharmcol. 59*, 506−513.
(50) Yu, D., Kazanietz, M. G., Harvey, R. G., and Penning, T. M. (2002) Polycyclic aromatic hydrocarbon *o*-quinones inhibit the activity of the catalytic fragment of protein kinase C. *Biochemistry 41*, 11888−11894.

TX0502488